ESC European Society of Cardiology
European Heart Journal - Cardiovascular Imaging (2019) **0**, 1–11
doi:10.1093/ehjci/jez046

Increased rotational flow in the proximal aortic arch is associated with its dilation in bicuspid aortic valve disease

Lydia Dux-Santoy[1†], Andrea Guala[1†], Gisela Teixidó-Turà[1], Aroa Ruiz-Muñoz[1], Giuliana Maldonado[1], Nicolás Villalva[1], Laura Galian[1], Filipa Valente[1], Laura Gutiérrez[1], Teresa González-Alujas[1], Augusto Sao-Avilés[1], Kevin M. Johnson[2,3], Oliver Wieben[2,3], Marina Huguet[4], David García-Dorado[1], Arturo Evangelista[1], and José F. Rodríguez-Palomares[1]*

[1]Department of Cardiology, CIBER-CV, Hospital Universitari Vall d'Hebron, Vall d'Hebron Institut de Recerca (VHIR), Universitat Autònoma de Barcelona, Passeig de la Vall d'Hebron 119–129, 08035 Barcelona, Spain; [2]Department of Medical Physics, University of Wisconsin-Madison, 1111 Highland Avenue, Madison, WI 53705-2275, USA; [3]Department of Radiology, University of Wisconsin-Madison, 600 Highland Ave, Madison, WI 53792, USA; and [4]Cardiac Imaging Unit, Pilar-Quirón Hospital, Carrer de Balmes 271, 08006 Barcelona, Spain

Received 10 September 2018; editorial decision 27 February 2019; accepted 28 February 2019

Aims Aortic dilation in bicuspid aortic valve (BAV) might extend to the proximal arch. Arch flow dynamics and their relationship with this segment dilation are still unexplored. Using 4D-flow cardiovascular magnetic resonance, we analysed flow dynamics in the arch for each BAV morphotype and their association with this segment dilation.

Methods and results One hundred and eleven BAV patients (aortic diameters ≤55 mm, non-severe valvular disease), 21 age-matched tricuspid aortic valve (TAV) patients with dilated arch and 24 healthy volunteers (HV) underwent 4D-flow. BAV were classified per fusion morphotype: 75% right-left (RL-BAV), and per arch dilation: 57% dilated, mainly affecting the right-noncoronary (RN) BAV (86% dilated vs. 47% in RL-BAV). Peak velocity, jet angle, normalized displacement, in-plane rotational flow (IRF), wall shear stress, and systolic flow reversal ratio (SFRR) were calculated along the thoracic aorta. ANCOVA and multivariate linear regression analyses were used to identify correlates of arch dilation. BAV had higher rotational flow and eccentricity than TAV in the proximal arch. Dilated compared with non-dilated BAV had higher IRF being more pronounced in the RN-morphotype. RN-BAV, IRF, and SFRR were independently associated with arch dilation. Aortic stenosis and male sex were independently associated with arch dilation in RL-BAV. Flow parameters associated with dilation converged to the values found in HV in the distal arch.

Conclusion Increased rotational flow could explain dilation of the proximal arch in RN-BAV and in RL-BAV patients of male sex and with valvular stenosis. These patients may benefit from a closer follow-up with cardiac magnetic resonance or computed tomography.

Keywords bicuspid aortic valve • 4D-flow cardiovascular magnetic resonance (4D-flow CMR) • aorta haemodynamics • aortic arch • aortic dilation

Introduction

Bicuspid aortic valve (BAV) is the most common cardiac congenital disease and is associated with a higher prevalence of aortic dilation than tricuspid aortic valve (TAV), with different dilation patterns associated with cusp fusion morphotypes.[1] The proximal ascending aorta (AAo) and the aortic root are the predominant areas of dilation in BAV patients. However, in some BAV patients the aortic dilation is

* Corresponding author. Tel: +34 (93) 2746212; Fax: +34 (93) 2746063. E-mail: jfrodriguezpalomares@gmail.com;jfrodrig@vhebron.net

† The first two authors contributed equally to this work and are joint first authors.

not confined to the AAo and it extends to the proximal aortic arch, with a reported prevalence of 23–73%.[2,3]

In clinical practice, echocardiography is the most used imaging technique in the assessment of aortic valve, aortic root, and proximal AAo.[4] However, echocardiography is not useful for visualizing distal AAo and proximal aortic arch (blind spots), which can only be analysed by computed tomography (CT) and cardiac magnetic resonance (CMR). Although both imaging techniques are indicated by current guidelines, the lack of ionizing radiation and the capacity to quantify blood velocity make CMR preferable for patients' follow-up.

The capacity of CMR to quantify three-dimensional blood velocity over time through 4D-flow sequences is particularly interesting in BAV aortopathy,[4–6] since altered flow dynamics may contribute to AAo dilation,[2,4,5,7–9] beyond genetic[10] and mechanical[11] causes, through extracellular matrix dysregulation and elastic fibre degeneration.[8] The influence of flow dynamics on aortic arch dilation has been analysed in few studies, which were limited to basic metrics.[7,12] More detailed knowledge of arch flow dynamics in BAV may help in identifying patients at higher risk of arch dilation who may benefit from closer follow-up with other imaging techniques beyond echocardiography, such as CMR or CT.

We aimed to analyse differences in the flow dynamic pattern in the aortic arch by 4D-flow cardiovascular magnetic resonance (4D-flow CMR), according to the valve morphotype and its association with proximal arch dilation in a large population of BAV patients. In addition, we analysed the relationship between altered flow dynamics (from the sinotubular junction to the distal descending thoracic aorta) and the extension of BAV aortopathy.

Methods

Study population

Between October 2014 and February 2017, 120 BAV patients aged >18 years were consecutively and prospectively recruited. Exclusion criteria were severe valvular disease and aortic root or AAo diameters >55 mm by echocardiography, uncontrolled hypertension, connective tissue disorders, aortic coarctation or other congenital heart diseases, and contraindication for CMR. In addition, 45 age-matched TAV [24 healthy volunteers (HV) and 21 patients with proximal aortic arch dilation with TAV] were prospectively enrolled with the same inclusion and exclusion criteria applied in BAV patients. The study was approved by the local ethics committee and written informed consent was obtained from all participants.

CMR protocol

CMR studies were performed on a 1.5 T Signa scanner (GE Healthcare, Waukesha, WI, USA). The protocol included double-oblique 2D bSSFP cine imaging to assess BAV morphotype, and 4D-flow acquisition with retrospective electrocardiogram-gating during free-breathing. Endovenous contrast was not given to minimize patient risk.

A radially-undersampled acquisition (PC-VIPR) with five-point balanced velocity encoding[13] was used for 4D-flow imaging of the entire thoracic aorta, with velocity encoding 200 cm/s, FOV $400 \times 400 \times 400$ mm^3, scan matrix $160 \times 160 \times 160$, flip angle 8°, TR 4.2–6.4 ms, and TE 1.9–3.7 ms. Reconstructions were performed offline to the nominal temporal resolution of each patient ($5 \times$ TR) with corrections for background phase errors from concomitant gradients and eddy currents, and for trajectory errors of the 3D radial acquired k-space.[14]

Data analysis: 4D-flow data processing

The thoracic aorta was semi-automatically segmented from an angiogram derived from 4D-flow and its centreline was computed using ITK-Snap. Co-registered 2D cine images were used to identify the sinotubular junction, supra-aortic vessels, and diaphragmatic level. Based on these locations, equidistant analysis planes orthogonal to the centreline were distributed in each of the three analysis regions: eight planes in the AAo (from the sinotubular junction to the brachiocephalic artery), four in the arch (from the brachiocephalic artery to the left subclavian artery), and eight in the thoracic descending aorta (from the left subclavian artery to diaphragmatic level). A reference point corresponding to the inner curvature of the aorta was defined on every contour to allow spatial registration among patients. For each plane, 3D velocity data were exported for calculations to be made using in-house Matlab code (MathWorks Inc, Natick, MA, USA). Peak-systolic parameters were averaged using one time-frame before and two time-frames after peak systole to mitigate noise, as in several studies.[5,7,15]

Flow parameters and wall shear stress

Maximum velocity magnitude, jet angle, normalized displacement, in-plane rotational flow (IRF), and vectorial wall shear stress (WSS) were obtained at peak systole as previously described.[9] Normal IRF values were established as those of HV (mean ± 2 SD).

Regional vectorial WSS was used to obtain WSS maps (64 points equally distributed for each section) and contour-averaged axial ($WSS_{ax,avg}$) and circumferential WSS ($WSS_{circ,avg}$)[9] (see *Figure 1*).

Dilation of the ascending aorta and the aortic arch

The AAo and the proximal aortic arch diameters were automatically measured using the 3D segmented thoracic aorta, as the best-fit diameter of the cross-sectional area at the levels of the pulmonary artery bifurcation and the brachiocephalic artery, respectively.

To determine the presence of AAo dilation, AAo diameter was adjusted with a logarithm transformation to set the *z*-score accounting for sex, age, and body surface area.[16] Dilation of the AAo was considered when *z*-score >2.[17] Arch dilation was considered when the measured diameter was greater than the expected diameter using the regression formulae by Hager *et al.*[18]

Statistical analysis

Continuous variables were expressed as mean ± standard deviation and assessed for normality using the Shapiro–Wilk test. Continuous variables were compared using Student's *t*-test if they presented a normal distribution and Mann–Whitney *U* test if they did not. Categorical variables were analysed with the χ^2 test.

Multivariate linear regression analysis with a backward selection procedure was used to evaluate relationships between demographic and flow variables and proximal arch dilation. Variables were entered into the model if $P < 0.25$[19] in univariate analyses.

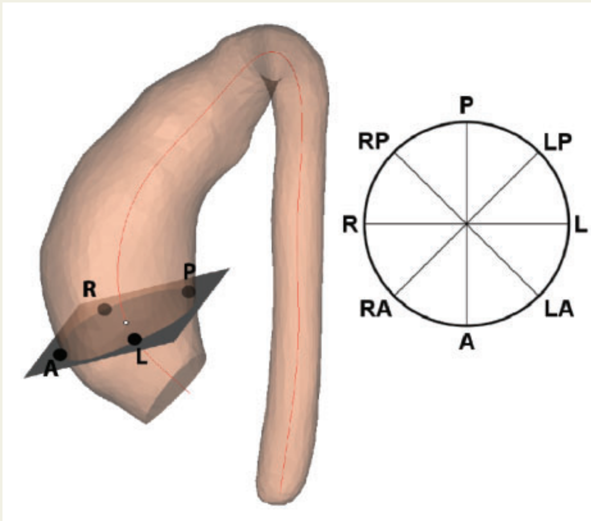

Figure 1 Regional WSS measurement regions. A, anterior; L, left; P, posterior; R: right.

A two-tailed *P*-value <0.05 was considered statistically significant. SPSS 19.0 (IBM SPSS Statistics, Chicago, IL, USA) was used for the analysis.

Results

Nine of the 120 BAV patients were excluded because of different reasons: claustrophobia ($n = 4$), connective tissue disorders unknown at the time of inclusion ($n = 1$), and suboptimal quality image for analysis ($n = 4$). The final study population comprised 111 BAV patients (83 RL and 28 RN-morphotype). BAV patients presented larger aortic diameters than TAV both at the sinus of Valsalva (SoV) ($P = 0.044$) and AAo ($P = 0.004$), higher diastolic arterial pressure ($P < 0.001$) and higher prevalence of aortic valve disease ($P < 0.001$ for regurgitation and $P = 0.004$ for stenosis) (see *Table 1*). No differences in aortic diameter were observed between RL and RN-BAV neither at the SoV (36.5 ± 4.9 mm vs. 35.4 ± 3.6 mm, $P = 0.286$) nor at the AAo (41.05 ± 7.7 mm vs. 41.3 ± 7.2 mm, $P = 0.853$). Arch dilation was present in 56.8% BAV, with a prevalence of 46.9% in RL-BAV and 85.7% in RN-BAV ($P < 0.001$). Among BAV patients with dilated AAo (*z*-score > 2) 67.3% presented aortic arch dilation. Seven (6.3%) BAV patients presented proximal arch diameter >40 mm. BAV patients with dilated aortic arch were older and had larger body size (see *Table 1*).

Patients with RL-BAV and aortic arch dilation were more likely to be male (79.5% vs. 50.0%, $P = 0.005$) and have mild-to-moderate stenosis (38.5% vs. 18.2%, $P = 0.040$) (see Supplementary data online, *Table S1*). In multivariate analysis, male sex ($P = 0.006$) and mild-to-moderate stenosis ($P = 0.039$) were independently associated with arch dilation in RL-BAV. Area under the ROC curve was 0.71.

Flow dynamics in the aortic arch

Results of flow analyses in the proximal and distal aortic arch are summarized in *Tables 2* and *3*. Results of the analyses in all slices are shown in Supplementary data online, *Tables S2* and *S3*.

Aortic arch flow dynamics and BAV morphotype

Flow rotation along the arch was right-handed in most HV (87.5%) and BAV (94.6%), both for RL and RN morphotypes. Abnormally-increased right-handed rotational flow (>84.6 cm^2/s, defined by mean + 2 SD in HV) was present in 21.6% RL-BAV and in 57.2% RN-BAV.

RN-BAV compared with RL-BAV patients presented significantly higher rotational flow (IRF) (*Figure 2B*) and $WSS_{circ,avg}$ at all arch levels ($P < 0.001$ for IRF and $WSS_{circ,avg}$ at proximal arch; $P = 0.013$ for IRF at the distal aortic arch), but similar flow displacement (*Figure 2A*, *Table 2* and Supplementary data online, *Table S2*).

Regional axial WSS maps were similar in both BAV morphotypes (*Figure 3A*), while circumferential WSS was significantly higher in RN-BAV in all aortic segments in distal AAo and proximal arch (*Figure 3*).

Aortic arch flow dynamics and arch dilation in BAV and TAV

Compared with HV, BAV patients with non-dilated arch presented higher IRF ($P < 0.05$) in the proximal arch and larger normalized displacement ($P < 0.05$) in the proximal and mid arch. All variables were similar between groups in the distal aortic arch except for normalized displacement ($P < 0.05$).

Dilated TAV compared with HV presented similar normalized displacement and rotational flow, but higher systolic flow reversal ratio (SFRR) and lower $WSS_{ax,avg}$ along the arch (*Table 3* and Supplementary data online, *Table S3*).

When comparing BAV according to arch dilation, dilated BAV had greater IRF and SFRR than non-dilated at all levels of the arch (*Figure 2D* and Supplementary data online, *Figure S1*), increased normalized displacement (*Figures 2C* and *4*) and lower $WSS_{ax,avg}$ at the proximal arch (*Table 3* and Supplementary data online, *Table S3*). Similar findings were observed in dilated compared with non-dilated RL-BAV (*Table 2* and Supplementary data online, *Table S2*), and in dilated compared with non-dilated RN-BAV. However, the reduced number of non-dilated RN did not allow for statistical comparison.

Regional axial WSS was decreased in dilated BAV (*Figure 5A*), while regional circumferential WSS was increased in dilated BAV in the anterior wall at proximal-mid aortic arch (*Figure 5B*).

In order to ascertain whether differences in flow in the aortic arch were a consequence of arch dilation or may play a causal role, dilated BAV were compared with age- and size-matched arch TAV patients. Dilated aortic arch in BAV compared with TAV still presented larger normalized displacement ($P < 0.001$) and higher rotational flow in the proximal and mid arch ($P < 0.001$ proximal arch; $P < 0.05$ mid arch for IRF and $WSS_{circ,avg}$) (*Table 3* and Supplementary data online, *Table S3*).

Multivariate correlated of proximal arch dilation in BAV

Significant unadjusted correlates of proximal arch dilation were BAV morphotype (RN-BAV), sex, height, and weight, in addition to increased rotational flow (IRF and SFRR) (see *Table 4*). On multivariate analysis RN-BAV, height, IRF, and SFRR were independently related to arch dilation.

In addition, the multivariate analysis was made considering the aortic arch diameter (as a continuous variable) and with the same clinical

Table 1 Demographics in TAV and BAV

	TAV			BAV		
	All ($n = 45$)	Healthy ($n = 24$)	Dilated arch ($n = 21$)	All ($n = 111$)	Non-dilated arch ($n = 48$)	Dilated arch ($n = 63$)
Age (years)	48.0 ± 16.0	44.8 ± 17.1	51.7 ± 14.1	50.9 ± 13.9	50.3 ± 14.0	51.4 ± 14.0
Men (%)	66.7	62.5	71.4	64	50	74.6[b]
Weight (kg)	73.6 ± 11.3	72.2 ± 10.9	75.0 ± 11.8	75.3 ± 13.1	70.2 ± 13.2	79.3 ± 11.6[b]
Height (cm)	170.2 ± 9.4	168.5 ± 9.5	172.0 ± 9.3	170.8 ± 9.7	167.3 ± 10.9	173.4 ± 7.7[b]
BSA (m^2)	1.85 ± 0.17	1.81 ± 0.16	1.88 ± 0.18	1.87 ± 0.20	1.79 ± 0.21	1.93 ± 0.16[b]
RL-BAV/RN-BAV				83/28	44/4	39/24[b]
Raphe (%)				68.8	68.8	68.9
Calcification (%)				48.8	45.9	51.0
Smoking (%)	24.4	20.8	33.3	9.2	8.1	10.0
Diabetes (%)	15.5	0.0	33.3	6.9	8.1	6.0
Aortic regurgitation degree (%)						
0	69.8[a]	100[a]	42.1[a,b]	15.3	17.4	13.5
1	20.9	0	36.8	76.5	78.3	75
2	9.3	0	21.1	8.2	4.3	11.6
Aortic stenosis degree (%)						
Absent	97.7[a]	100	94.7	71	80.4	63
Mild	0	0	0	18	8.7	25.9
Moderate	2.3	0	5.3	11	10.9	11.2
Systolic arterial pressure (mmHg)	131.9 ± 19.3	135.2 ± 21.7	127.1 ± 14.6[a]	136.2 ± 15.9	133.4 ± 13.7	138.3 ± 17.2
Diastolic arterial pressure (mmHg)	67.6 ± 12.6[a]	67.7 ± 13.0[a]	67.4 ± 12.3[a]	76.8 ± 9.1	75.0 ± 8.2	78.1 ± 9.6
SoV diameter (mm)	34.2 ± 7.1[a]	31.1 ± 4.5[a]	37.8 ± 7.9[b]	36.2 ± 4.6	34.3 ± 4.5	37.7 ± 4.3[b]
AAo diameter (mm)	36.3 ± 11.4[a]	29.6 ± 5.9[a]	44.2 ± 11.3[b]	41.1 ± 7.6	37.4 ± 7.1	43.9 ± 6.7[b]
Proximal arch diameter (mm)	29.1 ± 5.6	25.2 ± 3.2	33.5 ± 4.2[b]	30.8 ± 5.5	25.8 ± 3.1	34.6 ± 3.6[b]

Statistical significance ($P < 0.05$) comparing: [a]TAV vs. BAV counterpart, [b]dilated vs. non-dilated counterpart.

and flow variables (*Table 5*). This analysis confirmed the independent relationship between arch diameter and rotational flow parameters (IRF $P = 0.008$ and SFRR $P = 0.007$) as well as BAV morphotype (RN-BAV) ($P = 0.018$).

A schematic representation of flow parameters related to proximal arch dilation in BAV can be found in Supplementary data online, *Figure S1*.

Flow distribution in the thoracic aorta

Flow parameter distribution along the thoracic aorta (ascending, arch and descending) were compared for non-dilated and dilated arch BAV and HV (*Figure 6*). Compared with HV, BAV presented increased IRF, eccentricity, and SFRR in the AAo, extending to the proximal arch. These parameters were particularly increased in dilated compared with non-dilated aortic arch in BAV. In BAV, flow eccentricity (jet angle and displacement) and rotational flow parameters (IRF, $WSS_{circ,avg}$, and SFRR) presented their highest values in the AAo (reaching the maximum at mid-AAo) and decreased distally, converging along the mid-distal arch and proximal descending aorta and nearing values in HV (*Figure 6* and Supplementary data online, *Table S2*).

A change in direction of flow rotation in the descending aorta was observed in both BAV and HV, from right-handed flow in the AAo and arch (positive $WSS_{circ,avg}$ or IRF) to left-handed in the descending aorta (negative $WSS_{circ,avg}$ or IRF) (*Figure 6*).

Discussion

The main findings of this study were that proximal arch dilation was more prevalent in RN-BAV morphotype (86%) than in RL-BAV (47%); aortic stenosis and male sex are associated with arch dilation in RL-BAV patients, and BAV patients with proximal arch dilation showed higher rotational flow (IRF and $WSS_{circ,avg}$) than patients without arch dilation. The factors independently associated with proximal arch dilation are valvular morphotype (RN) and rotational flow parameters (IRF and SFRR).

Different studies have shown that altered flow dynamics may contribute to AAo dilation in BAV[5,7,9] through WSS-mediated degradation of the extracellular matrix and elastic fibres.[8] However, in some BAV patients with AAo dilation, the aortic enlargement also involves the proximal arch.[2,3] Thus, it is of interest to determine which factors may contribute to the extension of dilation to this segment, which

Table 2 Flow dynamics at proximal and distal arch per BAV-morphotype and arch dilation

	RL-BAV			RN-BAV		
	All (n = 83)	Non-dilated (n = 44)	Dilated (n = 39)	All (n = 28)	Non-dilated (n = 4)	Dilated (n = 24)
Vmax (cm/s)						
Proximal	103.08 ± 29.01	99.39 ± 27.48	107.23 ± 30.45	108.27 ± 33.24	100.74 ± 48.04	109.53 ± 31.37
Distal	98.50 ± 24.39	99.17 ± 24.57	97.75 ± 24.48	108.29 ± 47.19	97.62 ± 31.03	110.07 ± 49.65
Jet angle (°)						
Proximal	15.57 ± 7.45	14.83 ± 7.58	16.40 ± 7.30	16.05 ± 6.18	13.96 ± 6.76	16.40 ± 6.16
Distal	15.39 ± 6.16	15.83 ± 6.47	14.89 ± 5.84	14.78 ± 8.40	20.00 ± 20.13	13.92 ± 4.94
Normalized displacement						
Proximal	0.07 ± 0.03	0.06 ± 0.03[b]	0.08 ± 0.03	0.07 ± 0.02	0.05 ± 0.02	0.07 ± 0.02
Distal	0.06 ± 0.02	0.05 ± 0.02	0.06 ± 0.02	0.06 ± 0.02	0.05 ± 0.01	0.06 ± 0.02
IRF (cm^2/s)						
Proximal	54.73 ± 45.17[a]	44.13 ± 34.20[b]	66.69 ± 52.95	122.53 ± 103.97	53.32 ± 58.97	134.07 ± 106.14[b]
Distal	16.19 ± 15.88[a]	12.85 ± 14.89[b]	19.96 ± 16.31	31.50 ± 40.66	21.39 ± 19.60	33.18 ± 43.25
SFRR (%)						
Proximal	13.52 ± 11.92	8.58 ± 8.90[b]	19.09 ± 12.53	13.85 ± 7.10	9.95 ± 2.65	14.50 ± 7.43
Distal	6.21 ± 6.59	4.43 ± 4.95[b]	8.22 ± 7.62	7.15 ± 5.02	4.91 ± 3.33	7.53 ± 5.20
$WSS_{ax,avg}$ (N/m^2)						
Proximal	0.27 ± 0.16	0.32 ± 0.16[b]	0.21 ± 0.15	0.24 ± 0.12	0.19 ± 0.05	0.25 ± 0.12
Distal	0.41 ± 0.22	0.46 ± 0.22[b]	0.36 ± 0.22	0.35 ± 0.22	0.23 ± 0.07	0.37 ± 0.23
$WSS_{circ,avg}$ (N/m^2)						
Proximal	0.09 ± 0.07[a]	0.08 ± 0.06	0.09 ± 0.07	0.18 ± 0.15	0.07 ± 0.08	0.19 ± 0.15[b]
Distal	0.04 ± 0.04	0.03 ± 0.04	0.04 ± 0.03	0.06 ± 0.09	0.03 ± 0.04	0.07 ± 0.09

Statistical significance ($P < 0.05$) is indicated: [a]RL vs. RN-BAV, [b]compared with dilated RL-BAV.

presents clinical implications to determine the patients in whom the aortic surgery should encompass not only the AAo but also de proximal arch when this treatment option is considered. To our knowledge, this is the first study conducted in a large BAV population in which the persistence of abnormalities in flow dynamics in the proximal arch has been reported and related to local dilation, identifying which patients are at highest risk.

Aortic arch measurements

Most studies defining normality values for thoracic aorta diameters did not assess the aortic arch[1] and few studies have provided reference values for the this aortic segment,[18,20,21] but using different anatomical landmarks and imaging techniques. Consequently, there is no agreement in the definition of aortic arch dilation and predefined cut-off points have generally been used (30 or 40 mm).[2,7] Instead of using a predefined cut-off, we used an age-dependent threshold for proximal arch dilation based on the regression formula of Hager *et al.*[18] However, these normal values were not normalized by body dimension or sex. It is important to underline that multivariate analysis was also performed using proximal aortic arch diameter as a continuous variable, resulting in the identification of the same independent associations.

In our population, proximal arch dilation was present in 56.8% of BAV, mainly affecting the RN-BAV (86% dilated vs. 47.0% in the RL-BAV) as previously reported.[2,3,22] Other studies reported different prevalence of arch dilation in BAV, with dilated arch in 23.4–73% in the general BAV population,[2,3] 7–13% in RL-BAV, and 34.0–40.5% in RN-BAV.[2,7,23] The use of different imaging techniques (echocardiography, CT, or CMR) and predefined cut-off points in these studies could explain this variability. According to current guidelines, significant aortic dilation, defined as an aortic diameter >40mm,[1] was present in 6.3% of our BAV patients. Although arch dilation is related to AAo dilation,[2,3] only 67% of BAV patients with a dilated AAo presented a dilated aortic arch. Thus, other imaging markers beyond aortic diameter may contribute to identify patients at a higher risk.

Aortic arch flow dynamics in BAV

Previous studies reported the existence of eccentric[5,7] and increased rotational flow[5,15,24,25] in the AAo in BAV patients compared with TAV, leading to an increased aortic WSS with asymmetric regional distribution.[5,8,15,25,26] In our study, we observed that increased flow eccentricity and rotational flow still differed in the proximal and mid arch when BAV and TAV were compared, while other parameters (maximum velocity, SFRR, $WSS_{ax,avg}$) were similar.

This increased rotational flow was particularly high in the RN-BAV (coinciding with a higher rate of arch dilation), as previously reported in the AAo,[5] generating an increased circumferential WSS in all segments of the proximal arch. However, the differences in flow displacement between BAV morphotypes reported in the AAo[7,9] were

Table 3 Flow dynamics at proximal and distal aortic arch in BAV and TAV per arch dilation

	TAV			BAV		
	All (n = 45)	Healthy (n = 24)	Dilated (n = 21)	All (n = 111)	Non-dilated (n = 48)	Dilated (n = 63)
Vmax (cm/s)						
Proximal	106.58 ± 37.53	110.98 ± 31.70	101.55 ± 43.52	104.38 ± 30.06	99.50 ± 28.96	108.11 ± 30.57
Distal	103.40 ± 36.35	107.56 ± 32.75	98.63 ± 40.36	100.97 ± 31.75	99.04 ± 24.78	102.44 ± 36.31
Jet angle (°)						
Proximal	13.87 ± 4.97	14.16 ± 4.65	13.55 ± 5.42	15.69 ± 7.13	14.76 ± 7.45	16.40 ± 6.84
Distal	13.48 ± 4.70	14.01 ± 4.58	12.87 ± 4.87	15.24 ± 6.76	16.18 ± 8.10	14.52 ± 5.50
Normalized displacement						
Proximal	0.05 ± 0.02[a]	0.05 ± 0.02[a]	0.04 ± 0.01[a]	0.07 ± 0.03	0.06 ± 0.03	0.07 ± 0.03[b]
Distal	0.04 ± 0.01[a]	0.04 ± 0.02[a]	0.04 ± 0.01	0.06 ± 0.02	0.05 ± 0.02	0.06 ± 0.02
IRF (cm^2/s)						
Proximal	30.04 ± 34.93[a]	28.28 ± 27.92[a]	32.04 ± 42.19[a]	71.83 ± 71.06	44.90 ± 36.04	92.36 ± 83.58[b]
Distal	22.03 ± 25.26	20.58 ± 20.12	23.69 ± 30.53	20.05 ± 25.27	13.56 ± 15.26	25.00 ± 25.27[b]
SFRR (%)						
Proximal	10.50 ± 10.98	6.91 ± 8.73	14.60 ± 12.03[b]	13.60 ± 10.88	8.69 ± 8.55	17.34 ± 11.04[b]
Distal	5.42 ± 4.70	4.60 ± 4.09	6.36 ± 5.26	6.45 ± 6.22	4.47 ± 4.81	7.96 ± 6.77[b]
$WSS_{ax,avg}$ (N/m^2)						
Proximal	0.31 ± 0.19	0.38 ± 0.18	0.22 ± 0.18[b]	0.26 ± 0.15	0.31 ± 0.16	0.23 ± 0.14[b]
Distal	0.37 ± 0.20	0.43 ± 0.20	0.29 ± 0.18[b]	0.40 ± 0.22	0.44 ± 0.22	0.36 ± 0.22
$WSS_{circ,avg}$ (N/m^2)						
Proximal	0.05 ± 0.07[a]	0.05 ± 0.05	0.05 ± 0.08[a]	0.11 ± 0.10	0.08 ± 0.06	0.13 ± 0.12[b]
Distal	0.05 ± 0.05	0.05 ± 0.04	0.05 ± 0.06	0.04 ± 0.06	0.03 ± 0.04	0.05 ± 0.06

Statistical significance ($P < 0.05$) comparing: [a]TAV vs. BAV counterpart, [b]dilated vs. non-dilated counterpart.

not present in the proximal arch, thereby indicating they have similar velocity profiles at this level.

Determinants of aortic arch dilation in BAV

We found no differences between BAV with dilated and non-dilated arch in relation to the presence of raphe, valve calcification or hypertension, as also reported by Kang *et al.*[2] However, in the RL-BAV, previously related to root dilation,[23] arch dilation was associated with the presence of valvular stenosis[2,27] and male sex. We hypothesize that these clinical factors create flow alterations in RL-BAV like those in RN-BAV, promoting arch dilation. Similar to RN-BAV, male RL-BAV patients present increased distal AAo and aortic arch diameters that may contribute to perpetuate flow alterations at this level. Additionally, stenotic RL-BAV patients present a jet impinging the anterior wall of the distal AAo and the proximal arch, which causes an asymmetrical increase of WSS[28] and heterogeneous aortic wall degeneration contributing to dilation at this level.[8]

BAV patients with proximal arch dilation, mostly RN-BAV, presented increased rotational flow in the proximal arch, as occurs in the AAo.[5,9] However, this increased rotational flow was not observed when comparing dilated TAV and HV. These results may indicate that an excess in rotational and eccentric flow, resulting from the pathological aortic valve morphology, may play a causal role in dilation of the aortic arch, as suggested elsewhere.[5,9] Moreover, this rotational flow leads to an asymmetrically-increased circumferential WSS in the proximal arch of dilated BAV, which may contribute to aortic wall degradation and dilation as described in the AAo.[8]

Dilated BAV compared with non-dilated showed a larger normalized displacement in the proximal arch, thus indicating that increased eccentricity may also contribute to dilation as occurs in the AAo.[7,9] Although lower $WSS_{ax,avg}$ and higher SFRR were present in BAV patients with dilated arch, they were also observed in dilated TAV compared with HV and may thus be a consequence of dilation.[29]

The independent association of vortical flow parameters (both in-plane IRF and through-plane SFRR) together with valvular morphotype (RN) with proximal arch dilation in BAV was confirmed in the multivariate analysis.

Aortic flow and BAV aortopathy extension

We reported predominantly right-handed rotational flow in the AAo and arch in BAV patients and HV, with changed to left-handed rotation in the thoracic descending aorta. This behaviour has been previously reported in healthy subjects,[30,31] with the change in direction of

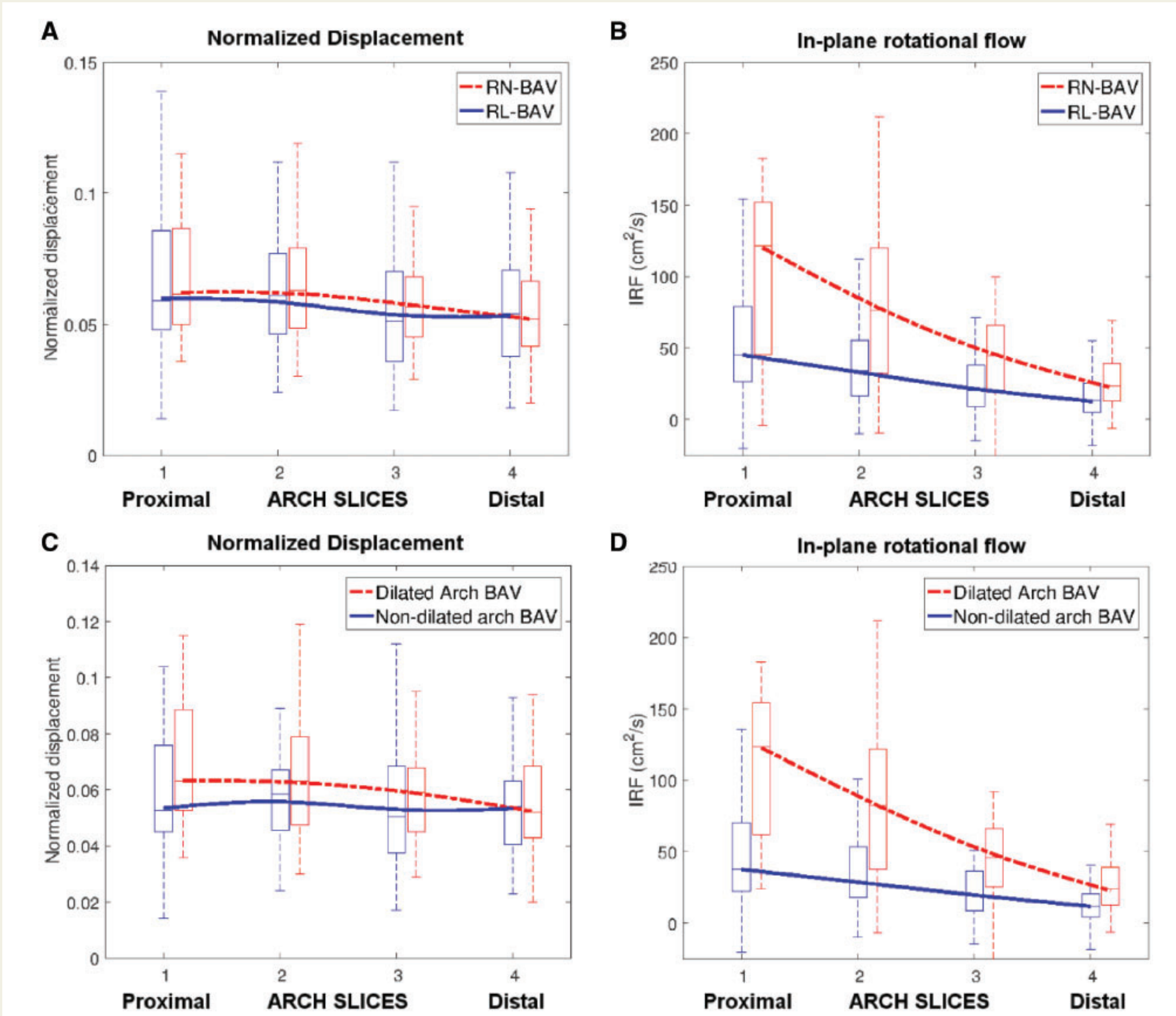

Figure 2 Normalized displacement and in-plane rotational flow in BAV per BAV morphotype (*A* and *B*) and arch dilation (*C* and *D*).

rotation in the thoracic descending aorta being attributed to the distal arch curvature.[30]

The distribution of flow parameters along the thoracic aorta revealed that differences in flow variables associated with dilation converged to values similar to those characteristic of HV in the regions where dilation is unusual (distal aortic arch and thoracic descending aorta).[3] This result further supports the role of flow in aortic dilation and may confirm that the geometric alterations in BAV mainly affect the AAo and the proximal arch.

Imaging follow-up

Diagnosis and follow-up of BAV are based on transthoracic echocardiography.[1] However, this imaging technique does not permit the evaluation of the distal AAo and proximal aortic arch. Thus, a more complete evaluation of the AAo and the proximal-mid arch with advanced imaging techniques including local flow evaluation, such as CMR, could be beneficial for patients with a higher risk of arch dilation. Our study shows that RN-BAV and RL-BAV patients of male sex or with valvular stenosis may benefit from a closer imaging follow-up by CMR or CT.

Limitations

Owing to the cross-sectional nature of the study, the causal role of flow dynamics in the development of arch dilation needs to be determined in further longitudinal studies and confirmed with histological analysis. Also, the analysis is limited to the contribution of flow alterations to aortic arch dilation and other factors such as genetics and epigenetics (not included in the present work) may contribute to aortic dilation.

Most cases with arch dilation had mild dilation, similarly to the more proximal segments of the aorta. As dilation by itself

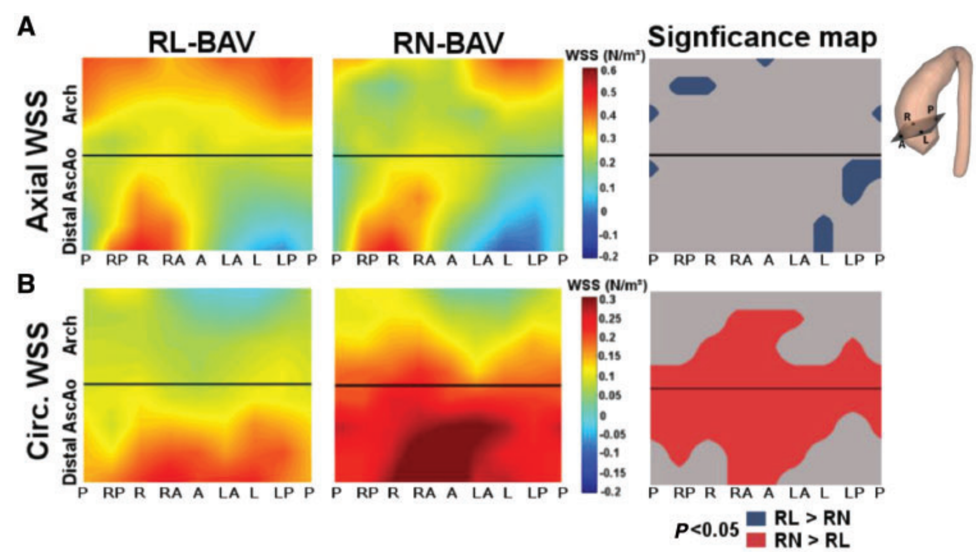

Figure 3 Regional WSS maps in the different BAV morphotypes and statistically significant difference ($P < 0.05$). (*A*) Axial WSS shows minimum differences. (*B*) Circumferential WSS is higher in RN-BAV at mid-distal ascending aorta and proximal-mid arch.

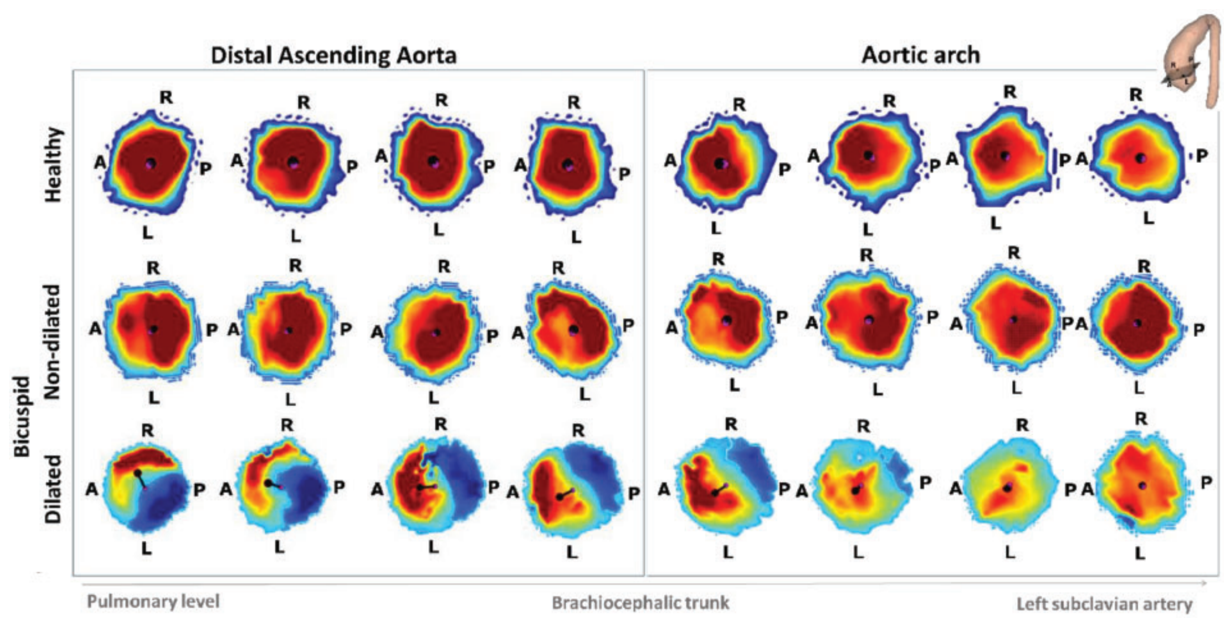

Figure 4 Flow displacement at the distal ascending aorta and aortic arch in a healthy volunteer and in BAV with non-dilated and dilated arch. Dilated BAV presents increased displacement.

may modify aortic biomechanical properties we preferred to investigate flow abnormalities in the contest of mild-moderate dilation.

Regional WSS maps computation may be affected by the heterogeneous location of the supra-aortic trunks and by the relatively limited number of analysis planes. Additionally, WSS is known to be underestimated owing to the low spatial and temporal resolutions of 4D-flow.[31,32] However, as all acquisitions were made using the same imaging parameters and analysed with the same methods, comparison between groups was unbiased. Although we have not performed a reproducibility test, the good inter- and intra-observer variability[33] and the good reproducibility over time[34,35] of flow and WSS measurements employed in this study have been previously demonstrated.

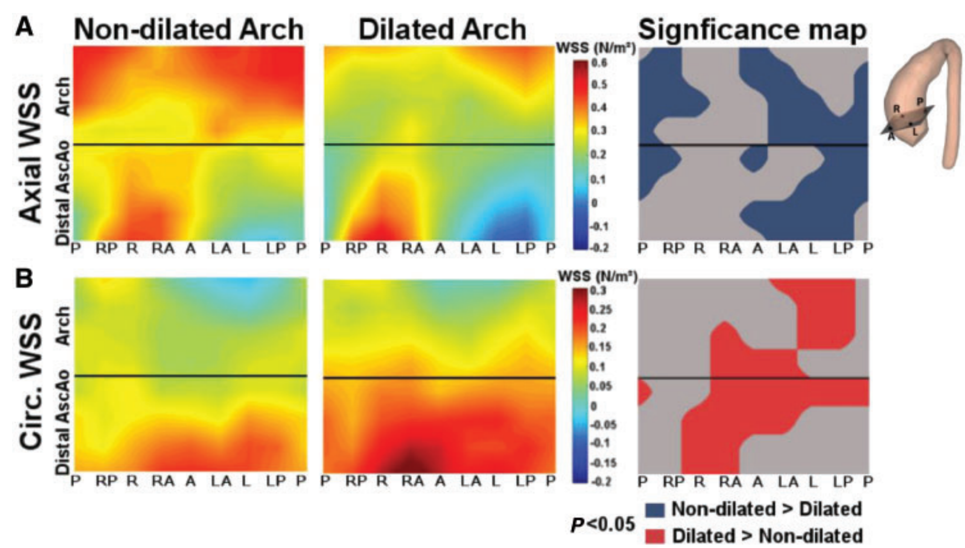

Figure 5 Regional WSS maps in BAV patients with dilated and non-dilated arch and statistically-significant difference ($P < 0.05$). (*A*) Axial WSS is regionally reduced in presence of dilation. (*B*) Circumferential WSS is increased in dilated BAV in anterior wall at proximal-mid arch.

Table 4 Unadjusted and adjusted relationship of demographic and local flow variables to proximal arch dilation

	Unadjusted correlates of arch dilation	Multivariate adjusted correlates of arch dilation		
	P-value	OR	95% CI	*P*-value
Sex (male)	0.007	2.57	0.61–10.83	0.198
height (cm)	0.001	1.11	1.045–1.182	**0.001**
Weight (kg)	<0.001	1.02	0.97–1.07	0.520
DBP (mmHg)	0.081	1.04	0.98–1.10	0.148
SBP (mmHg)	0.108	1.01	0.98–1.04	0.723
BAV morphotype (RN vs. RL)	<0.001	0.254	0.062–0.99	**0.049**
IRF (cm^2/s)	<0.001	1.014	1.002–1.027	**0.023**
SFRR (%)	<0.001	1.14	1.06–1.22	**<0.001**

P-values set in boldface indicate statistical significance ($P<0.05$) in the adjusted analysis.

Table 5 Unadjusted and adjusted relationship of demographic and local flow variables to proximal arch diameter

	Unadjusted correlates of arch diameter	Multivariate adjusted correlates of arch diameter	
	P-value	95% CI	*P*-value
Age (years)	0.001	0.06 to 0.19	**<0.001**
Sex (male)	0.014	-1.69 to 2.20	0.796
height (cm)	0.002	0.10 to 0.26	**<0.001**
Weight (kg)	<0.001	-0.09 to 0.07	0.836
DBP (mmHg)	0.053	0.01 to 0.18	**0.020**
SBP (mmHg)	0.030	-0.09 to 0.03	0.285
BAV morphotype (RN vs. RL)	0.001	0.99 to 4.64	**0.003**
IRF (cm^2/s)	0.013	0.00 to 0.03	**0.028**
SFRR (%)	<0.001	0.15 to 0.29	**<0.001**

P-values set in boldface indicate statistical significance ($P<0.05$) in the adjusted analysis.

Conclusions

Proximal aortic arch dilation is a common finding in BAV patients and mostly associated with the fusion of right and non-coronary leaflets. Aortic dilation at this level is associated with an increased rotational flow, however, other factors such as male sex and aortic stenosis may also contribute as risk factors. These patients may benefit from a closer follow-up with CMR or CT to determine those in whom the aortic surgery should encompass not only the ascending aorta but also the proximal arch when this treatment option is considered.

Supplementary data

Supplementary data are available at *European Heart Journal - Cardiovascular Imaging* online.

Acknowledgements

We would like to thank Christopher François (University of Wisconsin-Madison) and Rob van der Geest (Leiden University Medical Center) for advice on 4D-flow sequences, and Roberto García Álvarez (GE Healthcare) for technical support. We are also grateful to Christine O'Hara for English revisions.

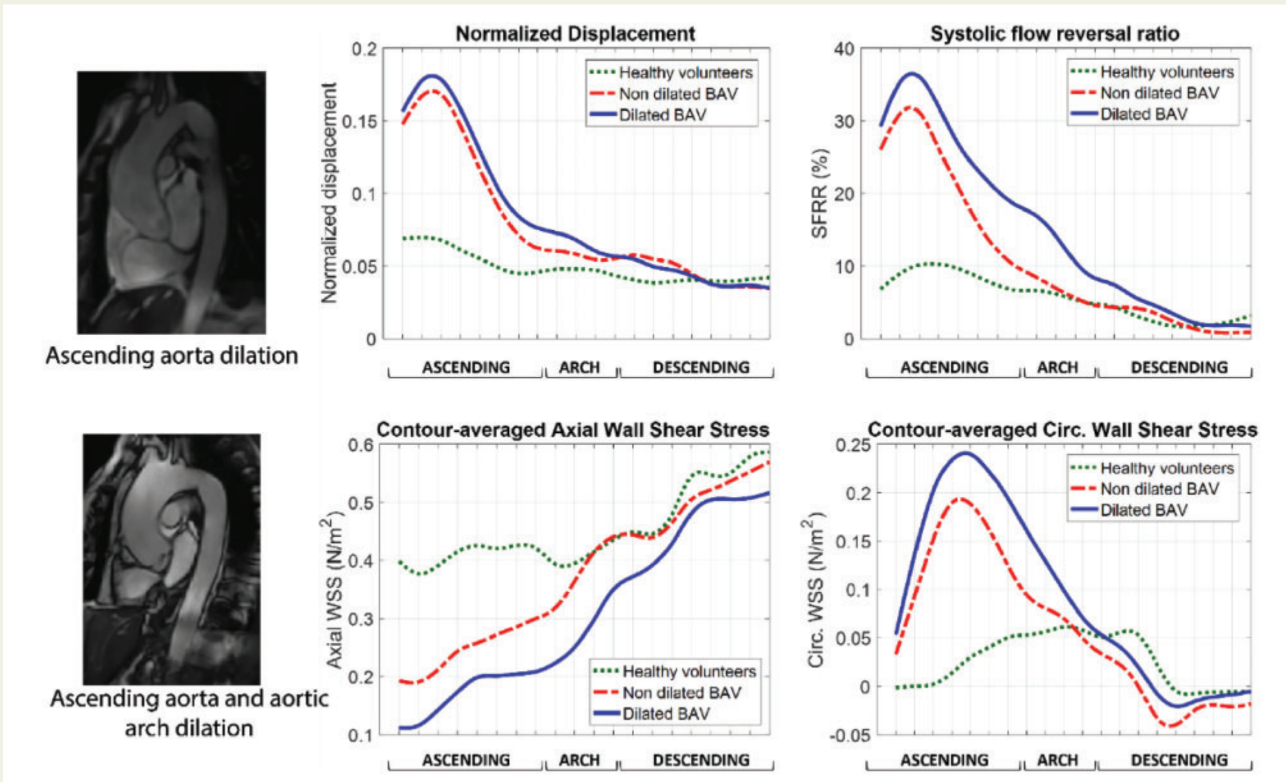

Figure 6 (Left) Examples of a patient with dilation of the ascending aorta (top) and of the ascending aorta and proximal aortic arch (bottom). (Right) Flow parameters along the thoracic aorta in HV and BAV per arch dilation, showing differences in the ascending aorta and proximal arch. Dilated BAV presented higher displacement, systolic flow reversal ratio and contour-averaged WSS than non-dilated BAV, but reduced axial WSS.

Funding

This study was funded by Instituto de Salud Carlos III through the project PI11/01081, La Marató de TV3 (project number 20151330), Ministerio de Economía y Competitividad through Retos-Colaboración 2016 (RTC-2016-5152-1), Beca Philips de la Societat Catalana de Cardiologia 2017 and CIBER-CV. A.G. received funding from the European Union Seventh Framework Programme FP7/People under grant agreement n° 267128.

Conflict of interest: K.M.J. has received a research grant from GE Healthcare and from Myocardial Solutions through The University of Wisconsin-Madison (no personal compensation) and holds a consulting agreement with Vertex Pharmaceuticals. O.W. has received a research grant from GE Healthcare through The University of Wisconsin-Madison (no personal compensation). All other authors have reported that they have no relationships relevant to the contents of this paper to disclose.

References

1. Erbel RA, Aboyans V, Boileau C, Bossone E, Di Bartolomeo R, Eggebrecht H *et al*. 2014 ESC guidelines on the diagnosis and treatment of aortic diseases. *Eur Heart J* 2014;**35**:2873–926.
2. Kang JW, Song HG, Yang DH, Baek S, Kim DH, Song JM *et al*. Association between bicuspid aortic valve phenotype and patterns of valvular dysfunction and bicuspid aortopathy: comprehensive evaluation using MDCT and echocardiography. *JACC Cardiovasc Imaging* 2013;**6**:150–61.
3. Fazel SS, Mallidi HR, Lee RS, Sheehan MP, Liang D, Fleischman D *et al*. The aortopathy of bicuspid aortic valve disease has distinctive patterns and usually involves the transverse aortic arch. *J Thorac Cardiovasc Surg* 2008;**135**:901–7.
4. Hope MD, Hope TA, Meadows AK, Ordovas KG, Urbania TH, Alley MT *et al*. Bicuspid aortic valve: four-dimensional MR evaluation of ascending aortic systolic flow patterns. *Radiology* 2010;**255**:53–61.
5. Bissell MM, Hess AT, Biasiolli L, Glaze SJ, Loudon M, Pitcher A *et al*. Aortic dilation in bicuspid aortic valve disease: flow pattern is a major contributor and differs with valve fusion type. *Circ Cardiovasc Imaging* 2013;**6**:499–507.
6. Stankovic Z, Allen BD, Garcia J, Jarvis KB, Markl M. 4D flow imaging with MRI. *Cardiovasc Diagn Ther* 2014;**4**:173–92.
7. Mahadevia R, Barker AJ, Schnell S, Entezari P, Kansal P, Fedak P *et al*. Bicuspid aortic cusp fusion morphology alters aortic three-dimensional outflow patterns, wall shear stress, and expression of aortopathy. *Circulation* 2014;**129**:673–82.
8. Guzzardi DG, Barker AJ, Van Ooij P, Malaisrie SC, Puthumana JJ, Belke DD *et al*. Valve-related hemodynamics mediate human bicuspid aortopathy: insights from wall shear stress mapping. *J Am Coll Cardiol* 2015;**66**:892–900.
9. Rodriguez-Palomares JF, Dux-Santoy L, Guala A, Kale R, Maldonado G, Teixidó-Turà G *et al*. Aortic flow patterns and wall shear stress maps by 4D-flow cardiovascular magnetic resonance in the assessment of aortic dilatation in bicuspid aortic valve disease. *J Cardiovasc Magn Reson* 2018;**20**:28.
10. Verma S, Siu SC. Aortic dilatation in patients with bicuspid aortic valve. *N Engl J Med* 2014;**370**:1920–9.
11. Guala A, Rodriguez-Palomares JF, Dux-Santoy L, Teixidó-Turà G, Maldonado G, Galian L *et al*. Influence of aortic dilation on the regional aortic stiffness of bicuspid aortic valve assessed by 4-dimensional flow cardiac magnetic resonance: comparison with Marfan syndrome and degenerative aortic aneurysm. *JACC Cardiovasc Imaging* 2018;doi:10.1016/j.jcmg.2018.03.017.
12. Raghav V, Barker AJ, Mangiameli D, Mirabella L, Markl M, Yoganathan AP. Valve mediated hemodynamics and their association with distal ascending aortic diameter in bicuspid aortic valve subjects. *J Magn Reson Imaging* 2018;**47**:246–54.
13. Johnson KM, Markl M. Improved SNR in phase contrast velocimetry with five-point balanced flow encoding. *Magn Reson Med* 2010;**63**:349–55.
14. Ibrahim EH, Johnson KR, Miller AB, Shaffer JM, White RD. Measuring aortic pulse wave velocity using high-field cardiovascular magnetic resonance: comparison of techniques. *J Cardiovasc Magn Reson* 2010;**12**:1–13.

15. Meierhofer C, Schneider EP, Lyko C, Hutter A, Martinoff S, Markl M *et al*. Wall shear stress and flow patterns in the ascending aorta in patients with bicuspid aortic valves differ significantly from tricuspid aortic valves: a prospective study. *Eur Heart J Cardiovasc Imaging* 2013;**14**:797–804.
16. Campens L, Demulier L, De Groote K, Vandekerckhove K, De Wolf D, Roman MJ *et al*. Reference values for echocardiographic assessment of the diameter of the aortic root and ascending aorta spanning all age categories. *Am J Cardiol* 2014;**114**:914–20.
17. Evangelista A, Gallego P, Calvo-Iglesias F, Bermejo J, Robledo-Carmona J, Sánchez V *et al*. Anatomical and clinical predictors of valve dysfunction and aortic dilation in bicuspid aortic valve disease. *Heart* 2018;**104**:566–73.
18. Hager A, Kaemmerer H, Rapp-Bernhardt U, Blücher S, Rapp K, Bernhardt TM *et al*. Diameters of the thoracic aorta throughout life as measured with helical computed tomography. *J Thorac Cardiovasc Surg* 2002;**123**:1060–6.
19. Mickey RM, Greenland S. The impact of confounder selection criteria on effect estimation. *Am J Epidemiol* 1989;**129**:125–37.
20. Agmon Y, Khandheria BK, Meissner I, Schwartz GL, Sicks JD, Fought AJ *et al*. Is aortic dilatation an atherosclerosis-related process? Clinical, laboratory, and transesophageal echocardiographic correlates of thoracic aortic dimensions in the population with implications for thoracic aortic aneurysm formation. *J Am Coll Cardiol* 2003;**42**:1076–83.
21. Mirea O, Maffessanti F, Gripari P, Tamborini G, Muratori M, Fusini L *et al*. Effects of aging and body size on proximal and ascending aorta and aortic arch: inner edge-to-inner edge reference values in a large adult population by two-dimensional transthoracic echocardiography. *J Am Soc Echocardiogr* 2013;**26**: 419–27.
22. Girdauskas E, Borger MA, Secknus MA, Girdauskas G, Kuntze T. Is aortopathy in bicuspid aortic valve disease a congenital defect or a result of abnormal hemodynamics? A critical reappraisal of a one-sided argument. *Eur J Cardiothorac Surg* 2011;**39**:809–14.
23. Della Corte A, Bancone C, Dialetto G, Covino FE, Manduca S, Montibello MV *et al*. The ascending aorta with bicuspid aortic valve: a phenotypic classification with potential prognostic significance. *Eur J Cardiothorac Surg* 2014;**46**:240–7.
24. Kolipaka A, Illapani VSP, Kalra P, Garcia J, Mo X, Markl M *et al*. Quantification and comparison of 4D-flow MRI-derived wall shear stress and MRE-derived wall stiffness of the abdominal aorta. *J Magn Reson Imaging* 2017;**45**:771–8.
25. Hope MD, Hope TA, Crook SES, Ordovas KG, Urbania TH, Alley MT *et al*. 4D flow CMR in assessment of valve-related ascending aortic disease. *JACC Cardiovasc Imaging* 2011;**4**:781–7.
26. Barker AJ, Markl M, Bürk J, Lorenz R, Bock J, Bauer S *et al*. Bicuspid aortic valve is associated with altered wall shear stress in the ascending aorta. *Circ Cardiovasc Imaging* 2012;**5**:457–66.
27. Della Corte A, Bancone C, Quarto C, Dialetto G, Covino FE, Scardone M *et al*. Predictors of ascending aortic dilatation with bicuspid aortic valve: a wide spectrum of disease expression. *Eur J Cardiothorac Surg* 2007;**31**:397–405.
28. Farag ES, van Ooij P, Planken RN, Dukker KCP, de Heer F, Bouma BJ *et al*. Aortic valve stenosis and aortic diameters determine the extent of increased wall shear stress in bicuspid aortic valve disease. *J Magn Reson Imaging* 2018;**48**: 522–30.
29. Bürk J, Blanke P, Stankovic Z, Barker A, Russe M, Geiger J *et al*. Evaluation of 3D blood flow patterns and wall shear stress in the normal and dilated thoracic aorta using flow-sensitive 4D CMR. *J Cardiovasc Magn Reson* 2012;**14**:84.
30. Kilner PJ, Yang GZ, Mohiaddin RH, Firmin DN, Longmore DB. Helical and retrograde secondary flow patterns in the aortic arch studied by three-directional magnetic resonance velocity mapping. *Circulation* 1993;**88**:2235–47.
31. Stalder AF, Russe MF, Frydrychowicz A, Bock J, Hennig J, Markl M. Quantitative 2D and 3D phase contrast MRI: optimized analysis of blood flow and vessel wall parameters. *Magn Reson Med* 2008;**60**:1218–31.
32. Dyverfeldt P, Bissell MM, Barker AJ, Bolger AF, Carlhäll C-J, Ebbers T *et al*. 4D flow cardiovascular magnetic resonance consensus statement. *J Cardiovasc Magn Reson* 2015;**17**:72.
33. Markl M, Wallis W, Harloff A. Reproducibility of flow and wall shear stress analysis using flow-sensitive four-dimensional MRI. *J Magn Reson Imaging* 2011;**33**: 988–94.
34. Van Ooij P, Powell AL, Potters WV, Carr JC, Markl M, Barker AJ. Reproducibility and interobserver variability of systolic blood flow velocity and 3D wall shear stress derived from 4D flow MRI in the healthy aorta. *J Magn Reson Imaging* 2016; **43**:236–48.
35. van der Palen RLF, Roest AAW, van den Boogaard PJ, de Roos A, Blom NA, Westenberg J. Scan-rescan reproducibility of segmental aortic wall shear stress as assessed by phase-specific segmentation with 4D flow MRI in healthy volunteers. *MAGMA* 2018;**31**:653–63.